

Active MHD Spectroscopy on the Resistive Wall Mode in DIII-D and JET

by

H. Reimerdest[†],

In collaboration with

M. Bigi[&], K.H. Burrell, M.S. Chu,
A.M. Garofalo[†], M.P. Gryaznevich[&],
T.C. Hender[&], D.F. Howell[&], G.L. Jackson,
R.J. La Haye, G.A. Navratil[†], M. Okabayashi^{*},
S.D. Pinches[#], J.T. Scoville, and E.J. Strait

[†]Columbia University

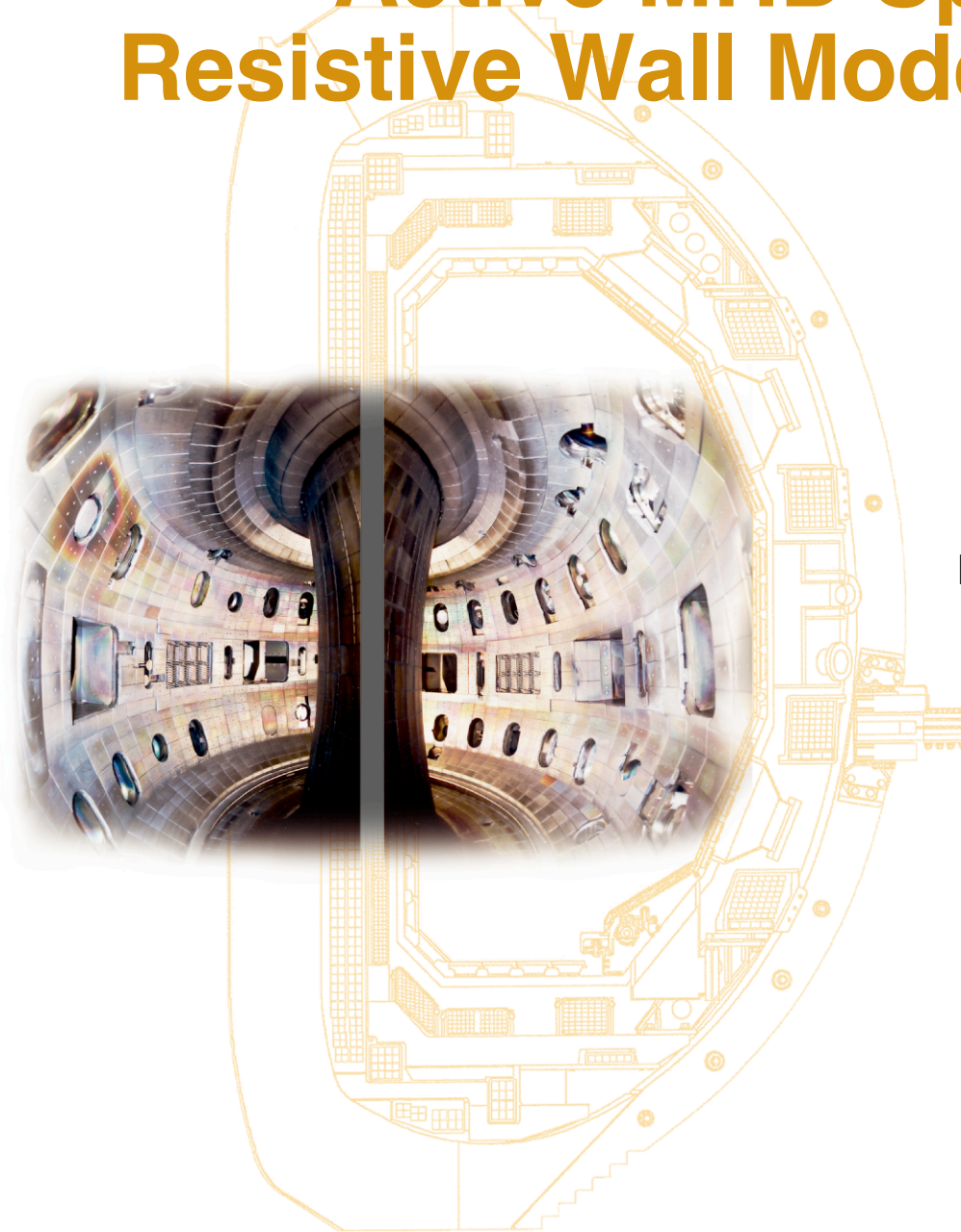
[&]EURATOM/UKAEA Fusion Association,

^{*}Princeton Plasma Physics Laboratory

[#]Max-Planck-Institut für Plasmaphysik

31st European Conference on
Plasma Physics and Controlled Fusion

June 28–July 2, 2004



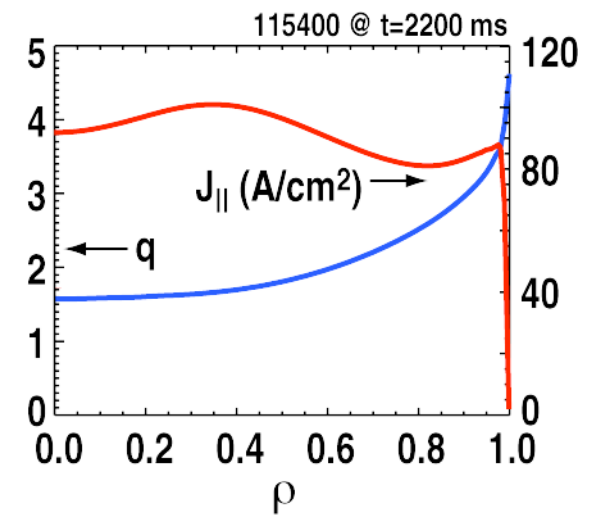
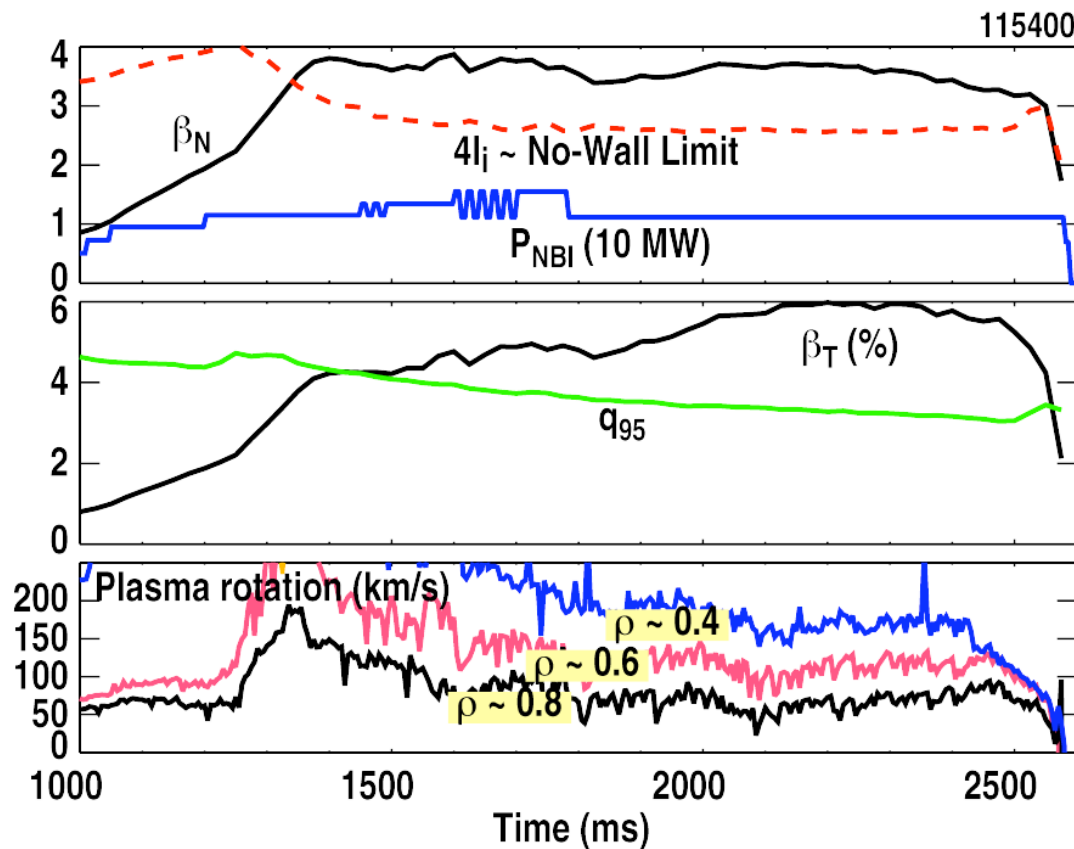
Outline

- Advanced tokamak operation with wall stabilization of the external kink mode
 - Dispersion relation of the resistive wall mode (RWM) and modifications due to plasma rotation
- Extend technique of active MHD spectroscopy to very low frequencies
 - Resonant field amplification (RFA)
- Frequency dependence of $n=1$ RFA in DIII-D
 - Description of RFA spectrum by a single mode approach
 - Measurement of the RWM growth rate and mode rotation frequency
- Frequency dependence of $n=1$ RFA in JET
- Application of active MHD spectroscopy
 - Test of sound wave dissipation model
 - Comparison of co- and counter NBI discharge
- Summary

Operation in the wall stabilized regime with $\beta_N \sim 6\text{li}$ and β_T reaching 6%

- Beta exceeds estimated no-wall limit for $>1\text{s}$.

- Broad current profiles can greatly benefit from wall stabilization.



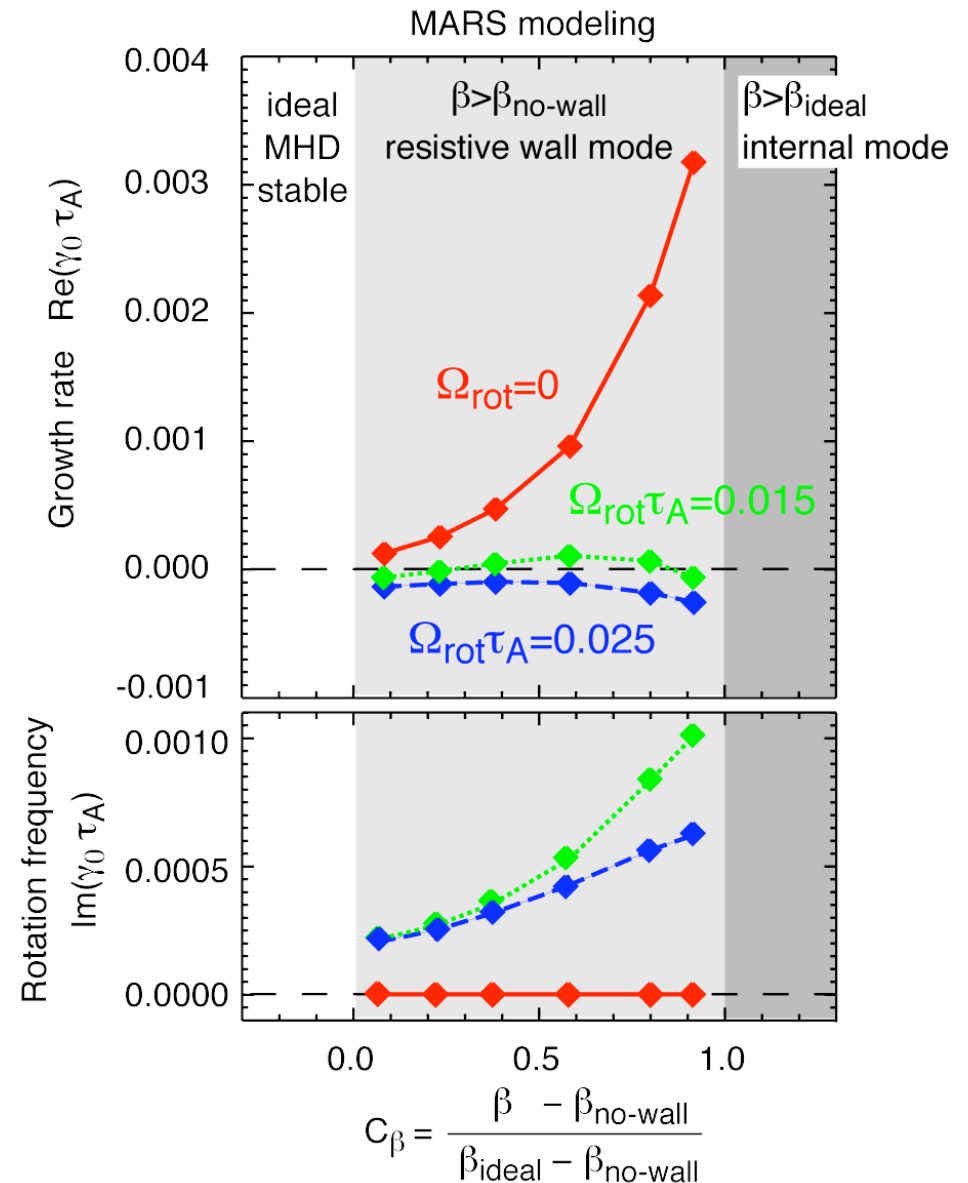
Stabilization of Resistive Wall Mode (RWM)

- **Resistive Wall mode (RWM):**

In the presence of a resistive wall, the free-boundary ideal MHD kink mode becomes a slowly growing RWM

- Observed between no-wall and ideal wall ideal MHD limit.
- “Slow” RWM growth $\gamma_{\text{RWM}} \sim \tau_w^{-1}$
→ Stabilization by feedback control.
- “Slow” mode rotation $\omega_{\text{RWM}} \ll \Omega_{\text{rot}}$
→ Quasi-static magnetic perturbation in a fast (toroidal) plasma flow.

Plasma flow and some **dissipation** alters linear stability [Bondeson and Ward, *Phys Rev Lett* **72** (1994) 2709].



Direct measurement of the RWM dispersion relation through active MHD spectroscopy

- **Active MHD spectroscopy**

Drive a low amplitude perturbation at various frequencies using external antennas and extract the plasma response with synchronous detection.

Example: Analysis of Alfvén eigenmodes in JET [Fasoli et al, *Phys Rev Lett* **74** (1995) 645]

- $\omega_{\text{ext}}/2\pi > 10^4$ Hz

- **Apply on Resistive Wall Mode** (where $\omega_{\text{RWM}} \sim 0$)

Understand interaction between external field and RWM (also important for feedback control), now for

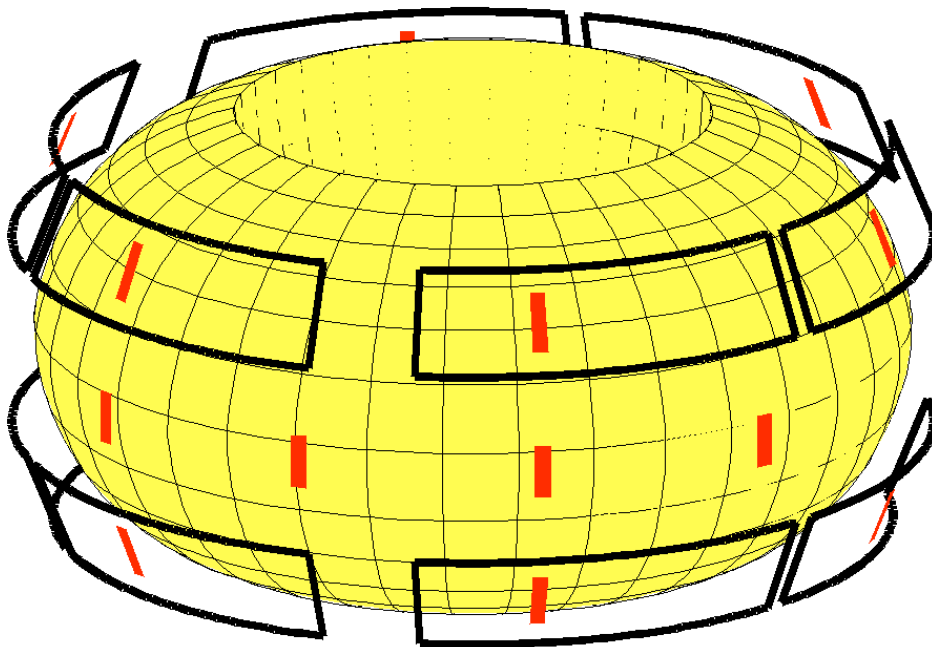
- $\omega_{\text{ext}}/2\pi < 100$ Hz, i.e. $\omega_{\text{ext}} \sim \tau_w^{-1}$, where τ_w is the characteristic decay time of wall eddy currents.

- **Resonant field amplification (RFA):**

External fields excite a marginally stable mode [Boozer, *Phys Rev Lett* **86** (2001) 1176].

- Dynamic response to externally applied resonant field pulses has been used to measure the RWM stability [Garofalo et al, *Phys Plasmas* **10** (2003) 4776].

DIII-D has versatile sets of antennas and detectors



Antenna:

- 12 internal saddle coils (I-coils).
- Phase coil currents to generate a **rotating magnetic field** with a large overlap with the **RWM structure** at the wall.

Detector:

- Toroidal arrays of saddle loops (and poloidal field probes) above, on and below the midplane.
- Frequency dependent vacuum coupling to I-coil is measured.

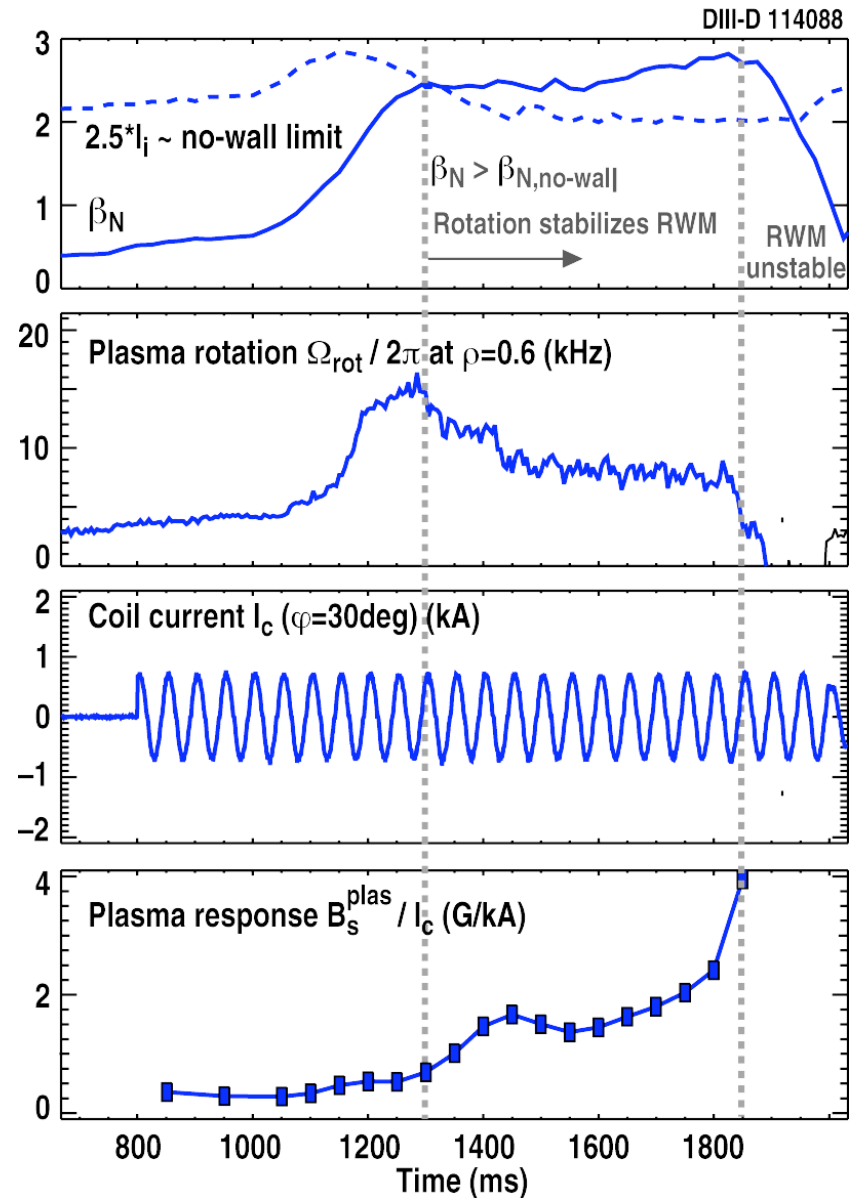
Rotating magnetic field applied to probe wall-stabilized DIII-D plasmas

- Apply a rotating low amplitude $n=1$ field:

$$I_c(t) = I_c e^{i\omega_{\text{ext}}t}$$

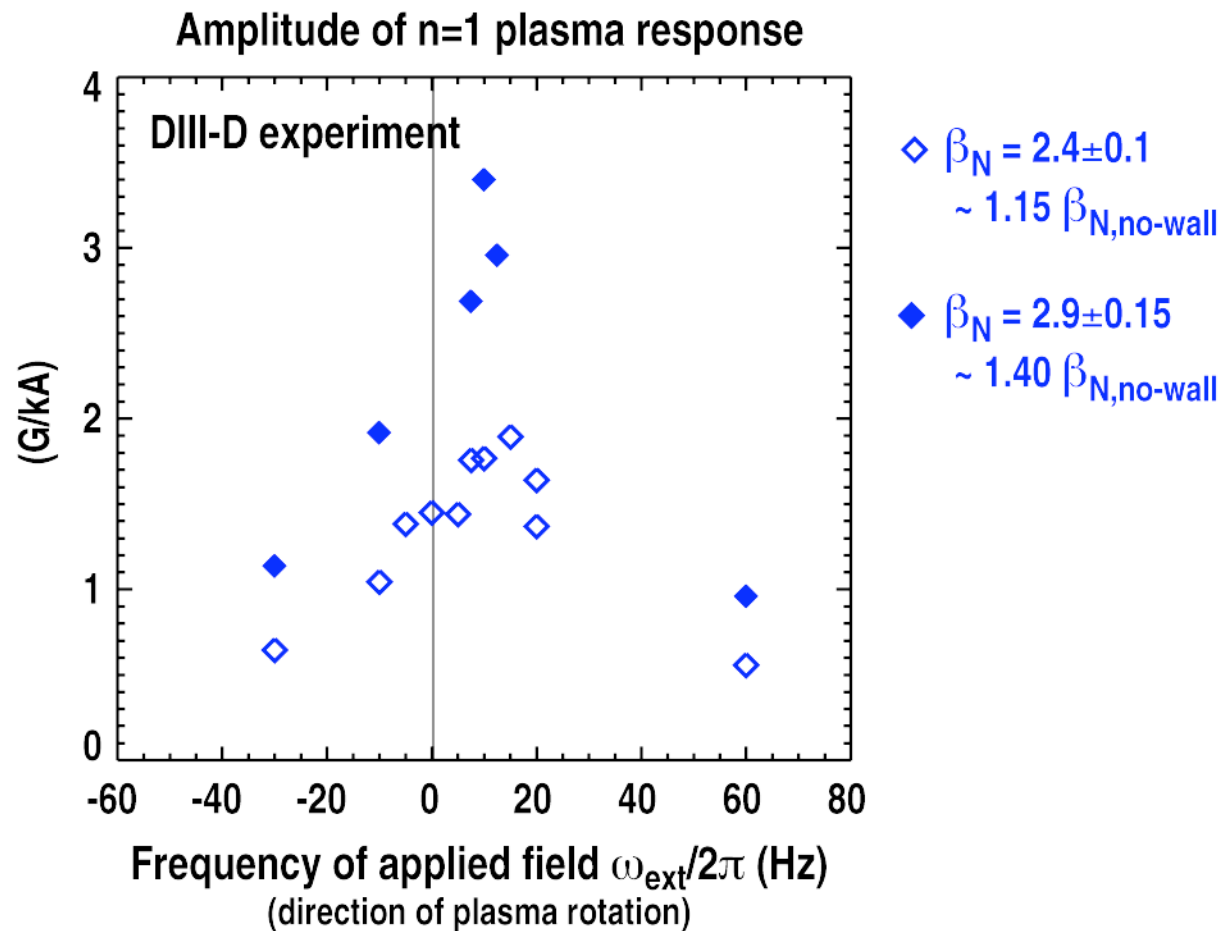
⇒ Plasma response increases significantly when beta exceeds the no-wall limit.

- Measure plasma response at different frequencies in multiple identical discharges.



Plasma response peaks for an externally applied field rotating in the direction of the plasma rotation

- Largest plasma response for $\omega_{\text{ext}}/2\pi \sim 10$ to 15 Hz, corresponding to $\omega_{\text{ext}} \sim 15$ to 25% of inverse wall time).
- Amplitude of plasma response increases with β .



Single mode model describes the interaction between the RWM and an externally applied field

- Single mode RWM model in slab geometry [Garofalo, Jensen, Strait, *Phys Plasmas* **9** (2002) 4573] yields relation between the perturbed radial field at the wall, B_s , and currents in the control coils, I_{ext} ,

$$\tau_w \frac{dB_s}{dt} - \gamma_0 \tau_w B_s = M_{sc}^* I_{ext}$$

- This expression holds for **general toroidal geometry** [Chu et al, *Nucl Fusion* **43** (2003) 196] and is **independent** of the details of the dispersion relation.
- Dispersion relations predict (complex) RWM growth rate, $\gamma_0 = \gamma_{RWM} + i \omega_{RWM}$, in the absence of external currents, e.g.:
 - **Ideal MHD with rotation and dissipation:** $\gamma_0 \tau_w$ from MARS calculations with various dissipation models [Liu, et al, *Phys. Plasmas* **7** (2000) 3681].

Single mode model predicts frequency dependence of the plasma response

- Distinguish between externally applied field and plasma response,

$$B_s = B_s^{plas} + B_s^{ext}$$

- Predicted plasma response to an externally applied field **rotating** with ω_{ext} :

$$B_s^{plas}(t) = \frac{\gamma_0 \tau_w + 1}{(i\omega_{ext} \tau_w - \gamma_0 \tau_w)(i\omega_{ext} \tau_w + 1)} M_{sc}^* I_c e^{i\omega_{ext} t}$$

- Here, M_{sc}^* is the **effective** mutual inductance describing the **resonant** component of the perturbed field at the wall due to coil currents I_c .

Measured spectrum consistent with predictions of a marginally stable RWM in a rotating plasma

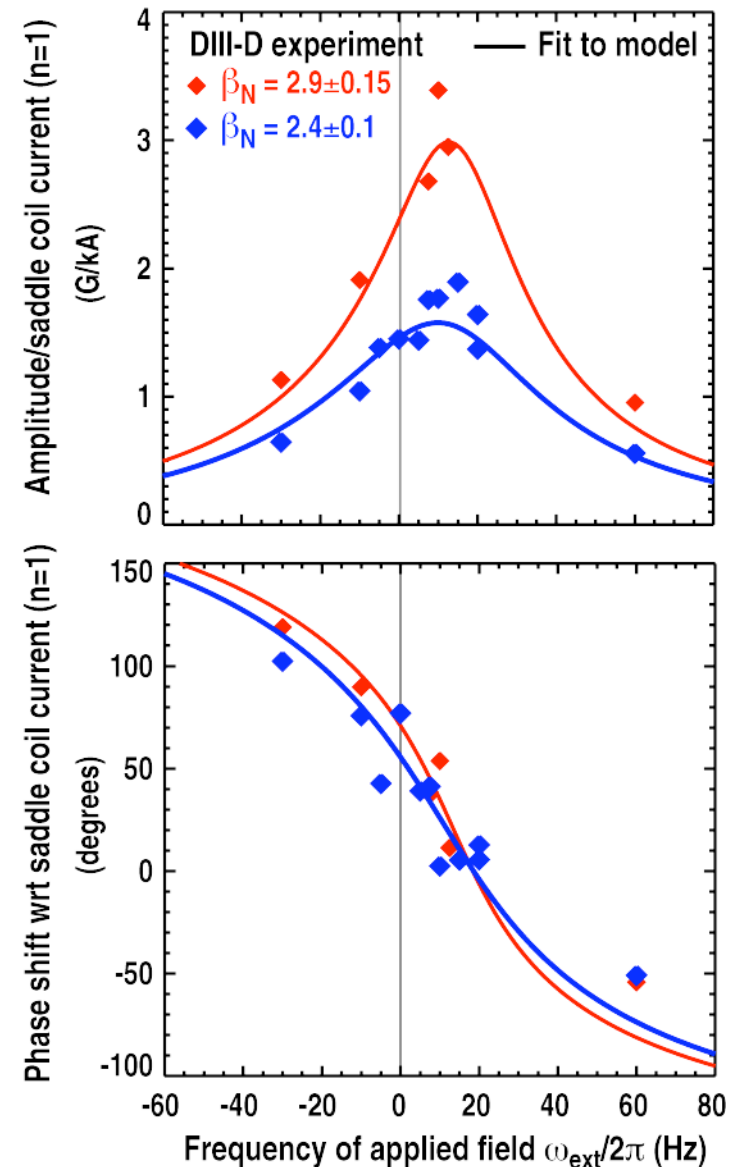
- Predicted frequency dependence of the plasma response,

$$B_s^{plas}(t) = \frac{\gamma_0 \tau_w + 1}{(i\omega_{ext} \tau_w - \gamma_0 \tau_w)(i\omega_{ext} \tau_w + 1)} M_{sc}^* I_c e^{i\omega_{ext} t}$$

- Fit γ_0 and M_{sc}^* to match measurements.
- Good agreement:
 - Indicates that a single-mode approach is applicable.
 - Yields measurement of the damping rate and mode rotation frequency:

$$\gamma_0 = (-157 + i80) \text{ s}^{-1} \text{ for } \beta_N = 2.4$$

$$\gamma_0 = (-111 + i73) \text{ s}^{-1} \text{ for } \beta_N = 2.9$$



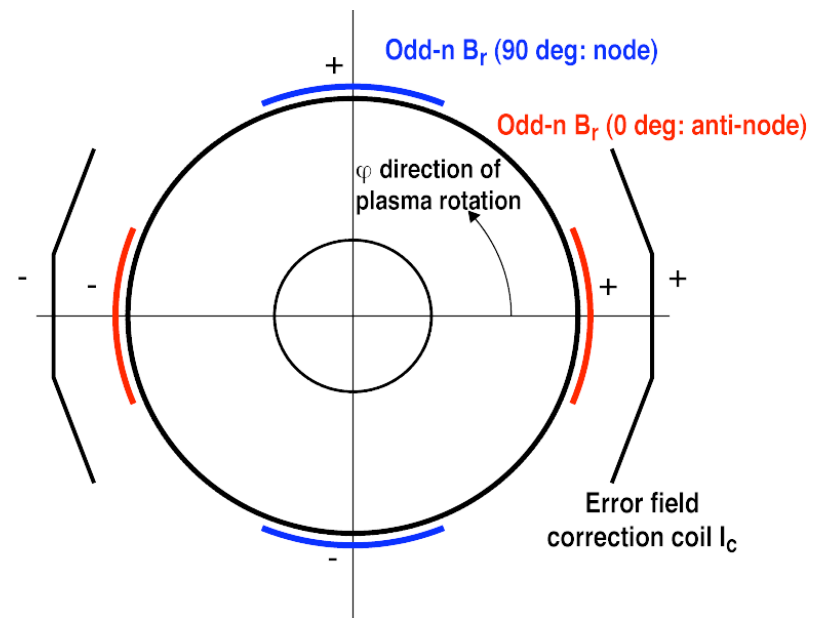
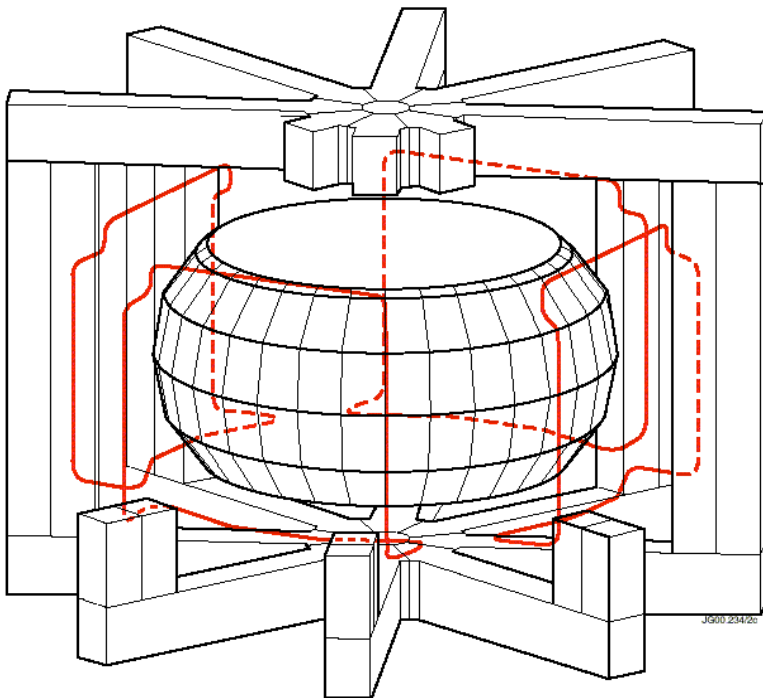
Measurement of the RFA spectrum on JET using the error field correction coils

Antenna:

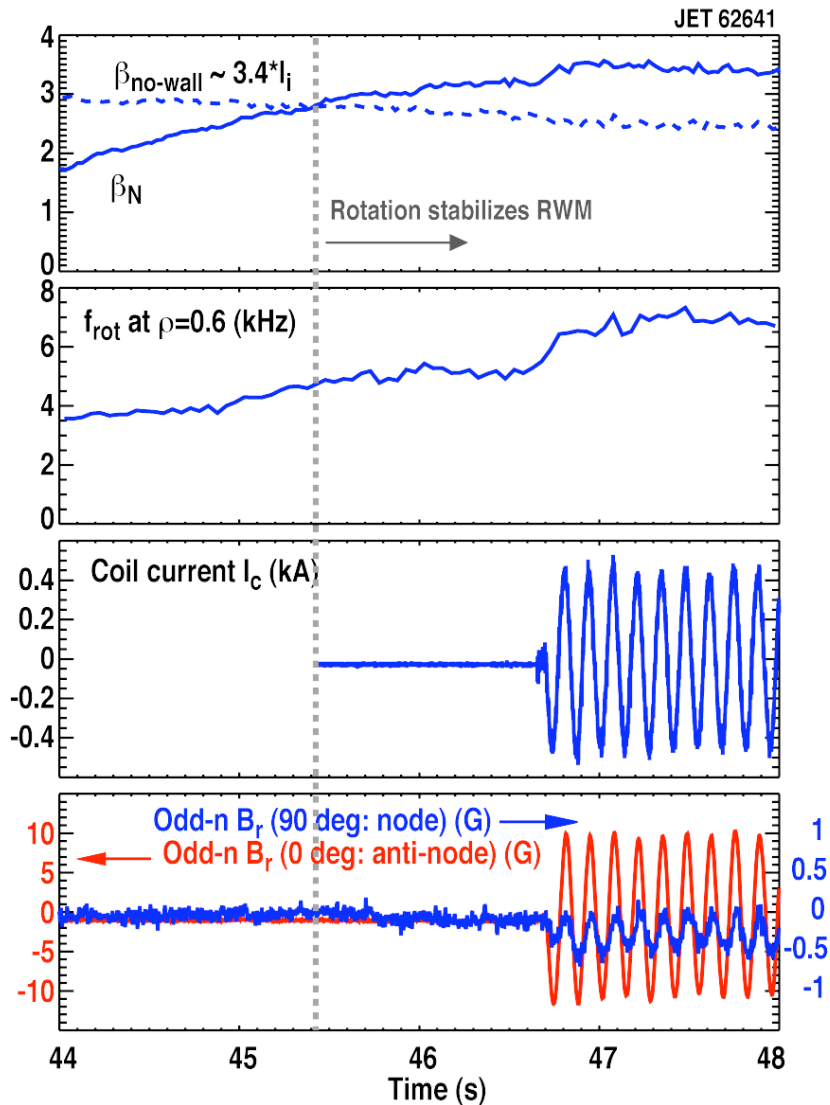
- One pair of the error field correction coils located in the midplane \Rightarrow apply $n=1$ pulses or standing waves.

Detectors:

- Two pairs of external odd- n B_r loops located at the **anti-node** and **node** of standing wave.



Standing wave applied to probe wall-stabilized JET plasmas



- Exceed the no-wall beta limit

- $B_T = 1.4\text{T}$

- $I_p = 1\text{MA}$

- $P_{\text{NBI}} \leq 20\text{MW}$

- $P_{\text{ICRH}} \leq 5\text{MW}$

- Apply an $n=1$ standing wave

$$I_c(t) = \frac{1}{2} I_c e^{i\omega_{\text{ext}} t} + \frac{1}{2} I_c e^{-i\omega_{\text{ext}} t}$$

- Odd-n B_r at the node shows a plasma response.

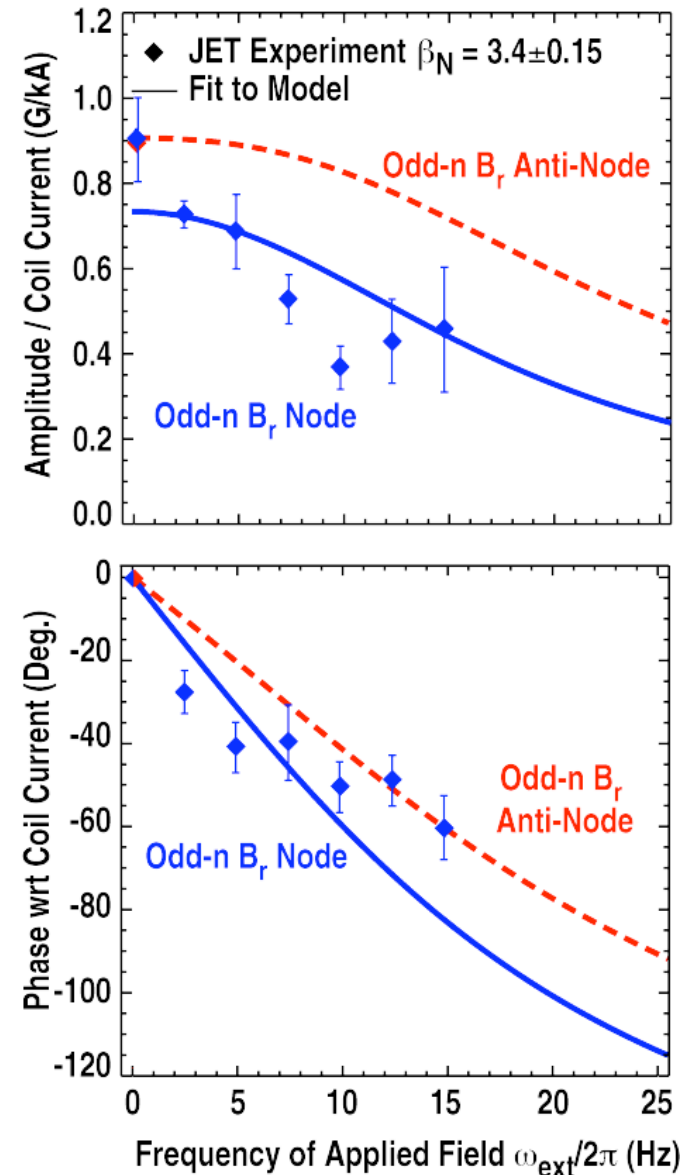
Frequency dependence of plasma response in JET consistent with the single mode prediction

- Large direct coupling to the anti-node sensor (30 times larger than B_s^{plas}) leads to a significant uncertainty of this measurement \Rightarrow use only data for 0 Hz.
- Measurements are consistent with the single mode approach:
 - Fit yields the damping rate and mode rotation frequency:

$$\gamma_0 = (-100 + i35) \text{s}^{-1} \text{ for } \beta_N = 3.4$$

- The values for $\gamma_0 \tau_w$ (with $\tau_w \sim 2.5$ ms in DIII-D versus $\tau_w \sim 5$ ms in JET) in both experiments are of similar magnitude,

$$\gamma_0 \tau_w \sim -0.4 + i 0.2 .$$



MHD spectroscopy yields a continuous - potentially real-time - measurement of global n=1 stability

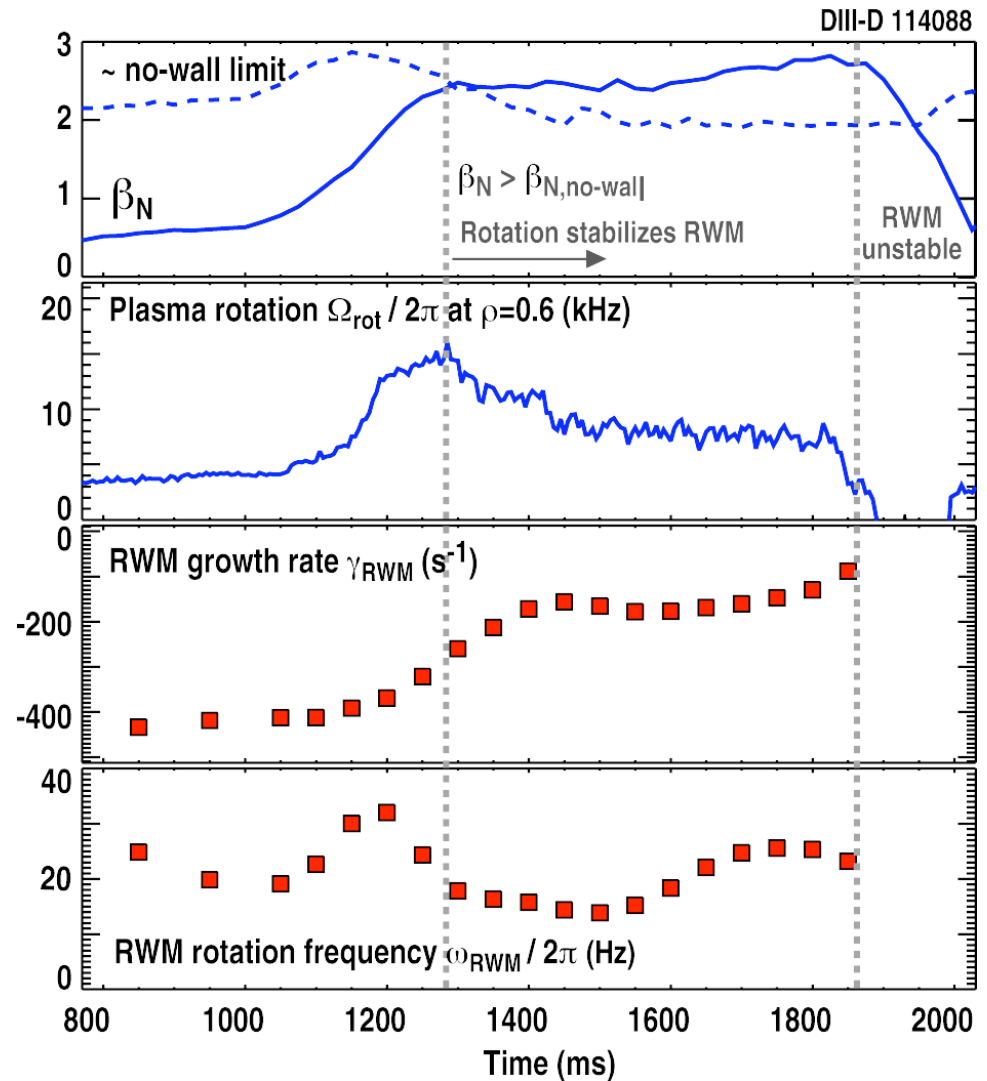
- With M_{sc}^* known from the fit of the entire spectrum the measurement of B_s^{plas} at a single frequency yields

$$\gamma_0 = \frac{i\omega_{ext} A_{RFA,S} / c_s - 1/\tau_w}{A_{RFA,S} / c_s + 1}$$

with $A_{RFA,S} = B_s^{plas} / B_s^{ext}$

and $c_s = M_{sc}^* / M_{sc}$

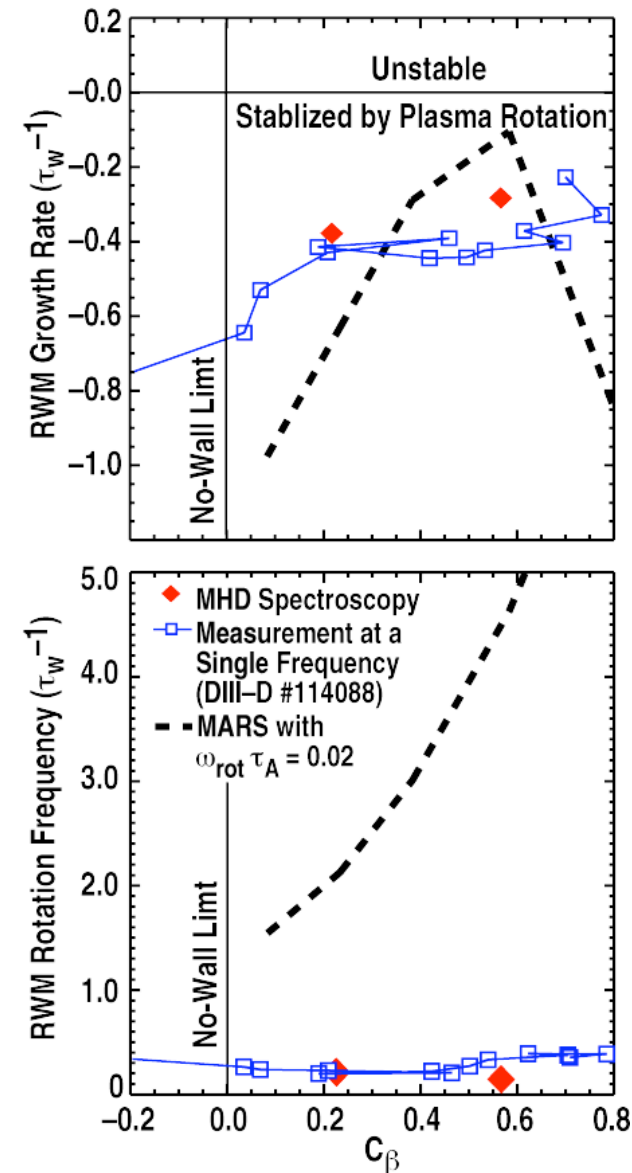
- Apply a low amplitude perturbation (300-700 A corresponding to 3-7 G at the antenna).



Measurement of RWM stability quantitatively tests dissipation models (MARS)

- First comparison with MARS code [Liu, et al, *Phys Plasmas* 7 (2000) 3681].
 - Generic equilibrium + DIII-D vessel + flat rotation profile + sound wave damping model.
- Observed damping rate is in good agreement with predictions
- Observed mode rotation frequency is an order of magnitude lower than predictions.

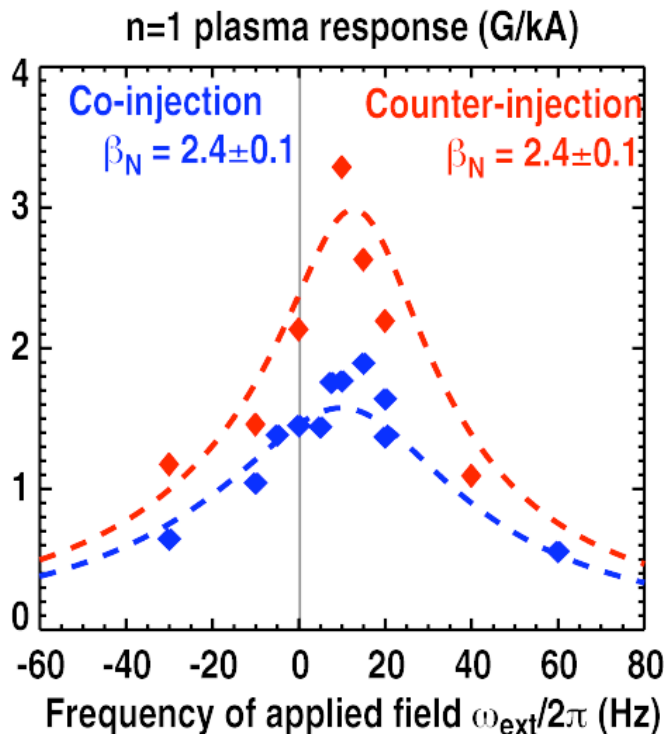
⇒ Further theoretical and experimental work is needed.



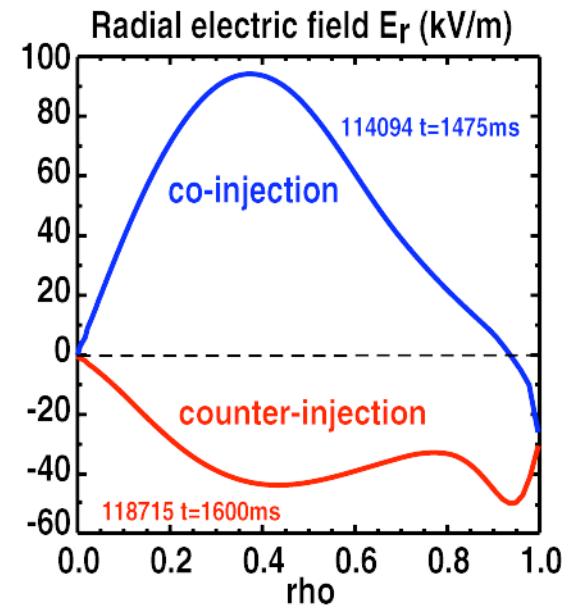
MHD spectroscopy allows investigation of models for RWM stabilization

Preliminary result

- Smaller plasma response indicates stronger damping with co-injection.



- Radial electric field varies.



Test predictions of dissipation mechanisms

- Soundwave damping [Bondeson and Ward]
- Kinetic damping [Bondeson and Chu]
- Neoclassical toroidal ripple viscosity [Shaing]
- Resonance with trapped particle precession [Hu and Betti]

Summary

- Interaction between externally applied resonant magnetic fields and the RWM in DIII-D and JET well described by a single marginally stable mode.
 - RFA spectrum yields measurement of the RWM damping rate and mode rotation frequency.
 - Extension of “Active MHD Spectroscopy” to very low frequencies.
 - Rotating fields can provides a continuous, potentially real-time, measurement of RWM stability.
 - Stability measurement allows for direct comparison with models of RWM stabilization by plasma rotation.
 - Comparison with soundwave-damping model shows qualitative agreement for damping rate, but observed mode rotation frequency is an order of magnitude lower than predictions
 - Different damping observed in co- and counter NBI discharges allowing test of predictions of stabilization models.
- ⇒ Further theoretical and experimental work is needed.